

Rain attenuation statistics over millimeter wave bands in South Korea

Sujan Shrestha, Dong-You Choi*

Department of Information and Communications Engineering, Chosun University, Republic of Korea



ARTICLE INFO

Keywords:

ITU-R P. 530-16

Millimeter wave communication

Rain attenuation

Rain rate

ABSTRACT

Rain induced degradations are significant for terrestrial microwave links operating at frequencies higher than 10 GHz. Paper presents analyses done on rain attenuation and rainfall data for three years between 2013 till 2015, in 3.2 km experimental link of 38 GHz and 0.1 km link at 75 GHz. The less link distance is maintained for 75 GHz operating frequency in order to have better recording of propagation effect as such attenuation induced by rain. OTT Parsivel is used for collection of rain rate database which show rain rate of about 50 mm/h and attenuation values of 20.89 and 28.55 dB are obtained at 0.01% of the time for vertical polarization under 38 and 75 GHz respectively. Prediction models, namely, ITU-R P. 530-16, Da Silva Mello, Moupfouma, Abdulrahman, Lin and differential equation approach are analyzed. This studies help to identify most suitable rain attenuation model for higher microwave bands. While applying ITU-R P. 530-16, the relative error margin of about 3%, 38% and 42% along with 80, 70, 61% were obtained in 0.1%, 0.01% and 0.001% of the time for vertical polarization under 38 and 75 GHz respectively. Interestingly, ITU-R P. 530-16 shows relatively closer estimation to measured rain attenuation at 75 GHz with relatively less error probabilities and additionally, Abdulrahman and ITU-R P. 530-16 results in better estimation to the measured rain attenuation at 38 GHz link. The performance of prominent rain attenuation models are judged with different error matrices as recommended by ITU-R P. 311-15. Furthermore, the efficacy of frequency scaling technique of rain attenuation between links distribution are also discussed. This study shall be useful for making good considerations in rain attenuation predictions for terrestrial link operating at higher frequencies.

1. Introduction

Rain induced attenuation can severely degrade the radio wave propagation at centimeter or millimeter wavelengths which restricts the path length of radio communication systems and limits the use of higher frequencies for line-of-sight microwave links. The rainfall results absorption and scattering of radio waves which result in the reduction of the received signal level. Above 10 GHz frequency liquid rain drops in the form of absorption and scattering become a serious contribute to transmission losses (Crane, 1996). When designing Line-of-Sight (LOS) microwave link or satellite link operating at frequency above 10 GHz, the occurrence of rain along the transmission path is considered as a main impairment factor for microwave system degradation (Freeman, 2007). The attenuation on any given path depends on the value of specific attenuation, frequency, polarization, temperature, path length and latitude (Kanellopoulos et al., 1990). It has created the need for balance between available bandwidth and rain attenuation at higher frequencies. Most attenuation prediction methods require the knowledge of 1 min rainfall rate statistics which in turn depends on the effective sampling time of the rain gauge (Mandeep

et al., 2008). Rainfall rate is the main factor in determining rain induced attenuation in a given link. The most widely used statistics are rain rate exceeded for a given percentage of the year which have taken into consideration of averages of statistics over many years due to the extreme variability of rainfall statistics at a given location (Barclay, 2003). The local prediction model is analyzed in the South Korea, where the modified polynomial model shows the predictable accuracy for estimation of 1 min rainfall rate distribution (Sujan et al., 2016; Shrestha et al., 2016; Sujan and Choi, 2016). In recent years, some location in the South Korea have experienced periods of unusually heavy rainfall which might be resulted due to urban heat island phenomena. This creates the interest to study the recent rain attenuation data measured in the South Korea which can be compared with the prominent rain attenuation methods (Choi et al., 2012). Rain attenuation prediction models take into account of path reduction factor, which features both path length and rainfall rate. The product of path reduction factor and the physical path length of a microwave link is the effective path length. It is observed that the effective path length is smaller than the actual physical path length, which leads to the introduction of path reduction factor (Islam et al., 2012). The method

* Corresponding author.

E-mail addresses: sujan.shrestha1@gmail.com (S. Shrestha), dychoi@chosun.ac.kr (D.-Y. Choi).

for the prediction of rain attenuation on microwave paths has been grouped into two categories (Kestwal et al., 2014): the empirical method, which is based on measurement databases from stations in different zones within a given region and physical method, which make an attempt to reproduce the physical behavior involved in the attenuation process. However, when a physical approach is considered then all the input parameters needed for the analysis is not available. Empirical method is therefore the most used methodologies (Crane, 2003). Rain attenuation effects have been studied worldwide and various models for solving the problem have been reported which are detailed in (Yussuff Abayomi, 2016; Kesavan et al., 2011; Mandeep, 2009; Abdulrahman et al., 2012a, 2011, 2016) that primarily focuses on the application of ITU-R P. 530-16. The rain attenuation statistics for higher microwave band wireless link were evaluated in Japan where the results agree well with the ITU model (Hirata et al., 2009). Six prominent rain attenuation models are considered for their suitability to local environment, namely, ITU-R P. 530-16 (ITU-R P. 530-16, 2015), Da Silva Mello et al. model (da Silva Mello et al., 2007; Mello and Pontes, 2012), Moupfouma's model (Moupfouma, 2009), Abdulrahman model (Abdulrahman et al., 2011), Lin model (Lin, 1977) and differential equations approach (Abdulrahman et al., 2012b). The rest of the paper is organized as follows: In "Background" section, we present a brief overview of applicable rain attenuation prediction models for terrestrial microwave link. "Analyses of Experimental data" describes the experimental setup which was used to demonstrate the procedure feasibility, followed by "Result and discussion" which summarizes the applicability of several models. Lastly, "Conclusion" concludes the paper and includes the suggestion for further research.

2. Background

Rain attenuation over a terrestrial path can be defined as the product of specific attenuation (dB/km) and the effective propagation path length (km) (Robert, 1996). The rain attenuation, A (dB) exceeded at p percent of time is calculated as:

$$A = \gamma_R d_{\text{eff}} = \gamma_R d * r \quad (1)$$

where, d_{eff} is the effective propagation path length which is the product of actual radio link, d in km and path reduction factor, r at the p time percentage.

The recommendation of the ITU-R P.838-3 (ITU-R, 2005) establishes the procedure of specific attenuation from the rain intensity. The specific attenuation, γ_R (dB/km) is obtained from the rain rate R (mm/h) exceeded at p percent of the time using the power law relationship as,

$$\gamma_R = kR^\alpha \quad (2)$$

where, k and α depends on the frequency and polarization of the electromagnetic wave. The constants appears in recommendation tables of ITU-R P. 838-3 (ITU-R, 2005) and also can be obtained by interpolation considering a logarithmic scale for k and linear for α . For the present location, values of two parameters at frequency 38 and 75 GHz under vertical polarization are obtained as $k=0.384403456$ and $\alpha=0.855219$; $k=1.099969083$ and $\alpha=0.711048$ respectively. Since the rainfall is not uniform along the propagation path, the effective propagation path length depends largely on the actual path length and reduction factor. The purpose of reduction factor is to reduce the actual path length filled with uniform point rainfall (COST, 255). Appendix A shows the applicable formulas for existing six rain attenuation models.

2.1. ITU-R P. 530-16

The ITU-R recommendation (ITU-R P. 530-16, 2015) suggests the path attenuation exceeded for 0.01% of the time as the product of

specific attenuation, γ_R (dB/km) and effective path length, d_{eff} for the consideration of time-space variability of rain intensity along the terrestrial path. The obtained value is scaled by the empirical formula to other percentages of time between 1% and 0.001% whose detail approach can be found in (ITU-R P. 530-16, 2015). This method is advised to be used in all parts of the world which stated that the rain attenuation needs to be considered for any operating frequency beyond 5 GHz and for frequencies up to 100 GHz with path lengths up to 60 km. This model is tested for link distance of operating frequencies 38 and 75 GHz under 3.2 and 0.1 km links respectively.

2.2. Da Silva Mello model

The model uses the numerical coefficients that are derived for effective rain rate and equivalent rain cell diameter that were obtained by multiple non linear regressions, using the measured data available in the ITU-R databanks (ITU-R Databank). Details of the model are fully reported in (da Silva Mello et al., 2007; Mello and Pontes, 2012). This approach retains the general expression for d_{eff} and uses the full rainfall rate distribution at the links region for 38 and 75 GHz operating frequencies of 3.2 and 0.1 km link distance as input for the prediction of the cumulative distribution of rain attenuation.

2.3. Moupfouma's model

This model is based on the use of rain intensity $R_{0.01}$ (mm/h) exceeded for 0.01% of the time, and the determination of the percentage of time related to the exceedence of any given attenuation of interest. This model is applied for 38 and 75 GHz links operating frequencies under link distance of 3.2 and 0.1 km respectively. The detail approach can be found in (Moupfouma, 2009).

2.4. Abdulrahman et al

This method studied the relationship between path reduction factor and different link lengths by using the multiple non-linear regression techniques. The link distance of 3.2 and 0.1 km are maintained for 38 and 75 GHz frequencies respectively so as to test the applicability of this method. Detail description of model can be obtained in (Abdulrahman et al., 2011).

2.5. Lin model

The method accounts for partially correlated rain rate variations along the propagation path length. This method is applied in the link distance of 3.2 and 0.1 km which are maintained for 38 and 75 GHz operating frequencies respectively. Further detailed explanation can be obtained in (Lin, 1977).

2.6. Differential equations approach

The method involves differentiation of measured rain attenuation with respect to rain rate. The results are presented in the form of slope, which in turn is used for predicting the expected rain attenuation at %p of the time on a 3.2 and 0.1 km link distance of 38 and 75 GHz operating frequencies respectively. The detail methodology is given in (Abdulrahman et al., 2012b).

3. Analyses of experimental data

The experimental data of rain attenuation and rain rate were collected in line-of-sight terrestrial links located in Icheon, South Korea for 38 and 75 GHz under vertical polarization, for three years period from 2013 till 2015. These data are obtained from National Radio Research Agency (RRA) and successive year's database is still under maintenance. The 38 GHz link is set between Khumdang

(37°08'8.41"N 127°30'56.16"E, Korea Telecom, KT station) tower and Icheon (37°08'49.57"N 127°32'54.82"E, National Radio Research Agency, RRA station) tower, at a separation distance of 3.2 km. Similarly, 75 GHz link is established between same Icheon tower and EMS Dong yoksang station (37°11'49.2"N 127°25'33.6"E), at a separation distance of 0.1 km. The climate in Icheon region is cold and temperate in which summers are much rainier than winters with average rainfall of 1296 mm/year (Korea Meteorological Administration). In 38 GHz link, one antenna at Khumdang, KT Station tower and next at Icheon, RRA Station tower in 3.2 km path length is vertically polarized. In addition, for 75 GHz operation in 0.1 km path length, one antenna at Icheon, RRA Station and next at EMS Dong yoksang Station is vertically polarized. These antennas were covered with radome to prevent wetting antenna conditions. The availability of transmitter and receiver system for 2013, 2014 and 2015 was 98.89%, 99.86%, 96.54% respectively. The downtime is resulted due to the calibration of receiver during clear sky days and power failures. Similarly, the uptime of the OTT Parsivel on 2013, 2014 and 2015 was 95.5%, 96.86%, 97.92% respectively. The downtime was because of the calibration and cleaning of the instrument. Their specifications are given in Tables 1 and 2.

The signal levels were sampled every 10 s and averaged over 1-min. The three years rainfall intensities with 99.95% of validity of all time were collected by OTT Parsivel which is an optical disdrometer for simultaneous measurement of particle size and velocity of precipitation types (Choi et al., 2012). The same disdrometer is used for rain rate measurement in satellite communication system as mentioned in (Shrestha and Choi, 2016). The disdrometer is a laser sensor which produces a horizontal strip of light where the emitter and receiver are integrated into a single protective housing. Whenever a hydrometeor falls through the laser beam then the measured signal output voltage changes which determine the particle size. Similarly, the duration of the signal determines the particle speed. Then disdrometer bin measured particles into particle counts per velocity and diameter class where there are 32 velocity and 32 diameter classes with varying widths. The rain rate is determined from the classification of precipitation particles. The ASDO software maintains the database of precipitation event. The sensor help to transmits all data to a PC through RS 485 interface. The automatic heating system prevents the ice buildup on the sensor heads which is adjusted by temperature sensor which measures the temperature each second. The detail list of procedure supported by Parsivel disdrometer can be found in (<http://www.ott.com>; OTT). The schematic diagram for system set up is shown in Fig. 1. As depicted in Fig. 1, one front-fed parabolic antenna is mounted on 35 m height Khumdang, KT Station tower for 38 GHz operations. The Out Door Unit (ODU) is connected to In Door Unit (IDU) via a 29 m coaxial cable. Similarly, two parabolic antennas are mounted on 20 m height Icheon, RRA Station tower under vertical polarization, for 38 and 75 GHz operations. The ODU of these antennas are connected to

Table 1
Specifications of the 38 GHz link (National Radio Research).

Descriptions	Specification
Antenna type	Front-fed Parabolic
Frequency band (for 38 GHz)	38.316 ~ 38.936
Polarization (@ Khumdang, KT station) tower	Vertical
Polarization (@ Icheon, RRA station) tower	Vertical
Maximum transmit power	0.063 W (+18 dBm)
Reception method	Super heterodyne
Modulation	QPSK
Maximum modulation degree	8 bit/Hz
BER received threshold (for vertical polarization) (dBm)	-29.8828
Half power beam width	0.9°
Antenna for both transmit and receive side	
Size (m)	0.6
Gain (dBi)	45.1

Table 2
Specifications of the 75 GHz link (National Radio Research).

Descriptions	Specification
Antenna type	Front-fed Parabolic
Frequency Band (for 75 GHz)	71 ~ 76
Polarization (@Icheon, RRA station) tower	Vertical
Polarization (@EMS Dong yoksang station) tower	Vertical
Maximum transmit power	0.005 W (+7 dBm)
Reception method	Super heterodyne
Modulation	QPSK
Maximum modulation degree	6 bit/Hz
BER received threshold (for vertical polarization) (dBm)	-22.9492
Half power beam width	0.8°
Antenna for both transmit and receive side	
Size (m)	0.6
Gain (dBi)	45.1

separate IDU via 46 m coaxial cable. Similarly, one front-fed parabolic antenna is maintained in EMS Dong yoksang Station Tower which is connected to IDU through ODU via 5 m coaxial cable since this station lies on roof top of the building. The data logger unit along with OTT Parsivel rain gauge is setup in Icheon, RRA Station where, rain gauge is set up at top of the tower.

The corresponding path attenuation is calculated by finding the difference between the RSL during clear sky conditions and the RSL during rain for horizontal and vertical polarized received signal at various rain rates as follows:

$$\text{Attenuation (dB)} = \text{RSL}_{\text{clear sky}} - \text{RSL}_{\text{rainy}} \quad (3)$$

Similar approach as for determining 1 min rain rate in (Choi et al., 2012) is adopted for calculating the rain attenuation value for 1 min interval. The cumulative distribution of 1 min rain rate calculated from the measured rain rate of 10 s intervals for three years (2013 till 2015) of the studied location is shown in Fig. 2. These data are sorted in descending order and the required 1 min rainfall rate, and attenuation values are determined from 1% to 0.001% of the time. For example, at 0.01% of the time, 1 min rain rate and attenuation values are taken for about 158 $((3 \times 365 \times 24 \times 60 \times 0.01) / 100) = 157.68 \approx 158$ instance for 3-years measurement when sorted together. This figure indicates that at 0.01% of the time the 1 min rain rate value is 49.79 mm/h for Icheon site. Furthermore, 1 min rain rate values decreases and tends to be smaller for higher time percentages, for example, at 0.5% and 1% of the time, the rain rate are observed to be 1.99 mm/h and 0.65 mm/h. Similarly, at lower time percentage 1 min rain rate is increased, for example, at 0.001% of the time the rain rate observed is 98.57 mm/h.

Fig. 3 depicts the plot of rain attenuation against rain rate for experimental links of 38 and 75 GHz which highlights the increment of attenuation values against the rain rate. Higher rain rate results in greater attenuation and prominent effect is observed in 75 GHz link. For instance, in 10.58, 49.79, 98.57 mm/h, the corresponding rain attenuation values are 10.53, 20.89, 38.44 dB and 16.11, 28.55, 40.48 dB under 38 and 75 GHz links under vertical polarization respectively.

4. Result and discussions

The complementary cumulative distribution of measured rain attenuation is compared with ITU-R P. 530-16 for several time percentages at equiprobable exceedance probability ($0.001\% \leq P \leq 1\%$) which are plotted in Fig. 4. Fig. 4 shows the rain attenuation at two different frequencies in which rainfall result in greater attenuation for 75 GHz as compared to 38 GHz and its values get increased for lower time percentage which reached up to 40.48 and 38.44 dB at 0.001% of the time respectively. Conversely, at higher time percentage as such for 1% of the time, the rain attenuation values get decreased to 1.01 and 0.41 dB respectively. The prediction of ITU-R P. 530-16

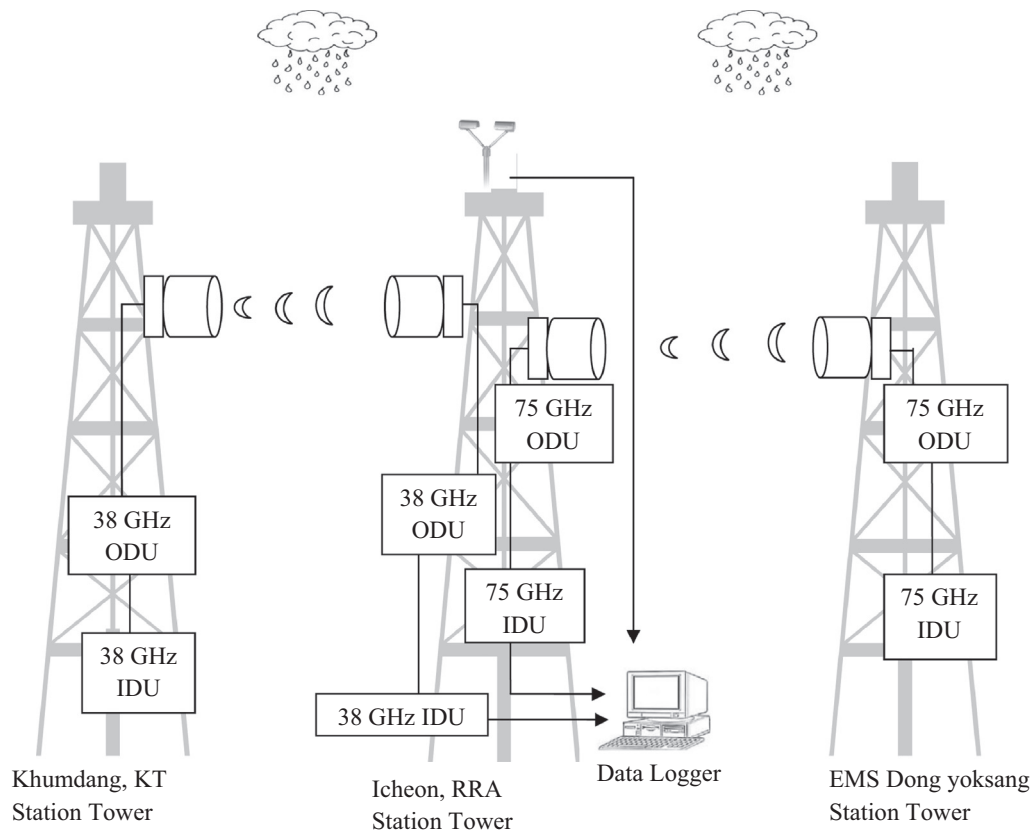


Fig. 1. Experimental setup for rain attenuation and rain rate measurement (National Radio Research).

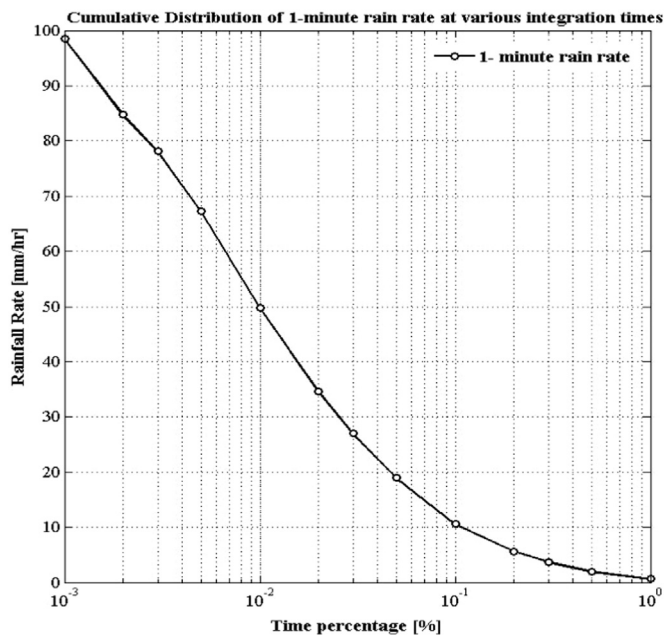


Fig. 2. Rainfall rate distribution of various integration times (National Radio Research).

shows the underestimation with greater deviation against the measured values of approximately 20 dB at 75 GHz link. The reason behind this difference might be due to the fact that the parameters used to obtain the rain attenuation from ITU-R P. 530-16 have not considered the propagation effects such as rain drop size distributions which might show large drop density at smaller sizes. Additionally, ITU-R P. 530-16 considers additional propagation effects such as atmospheric gases, sand storm, diffraction effect which might have resulted in greater

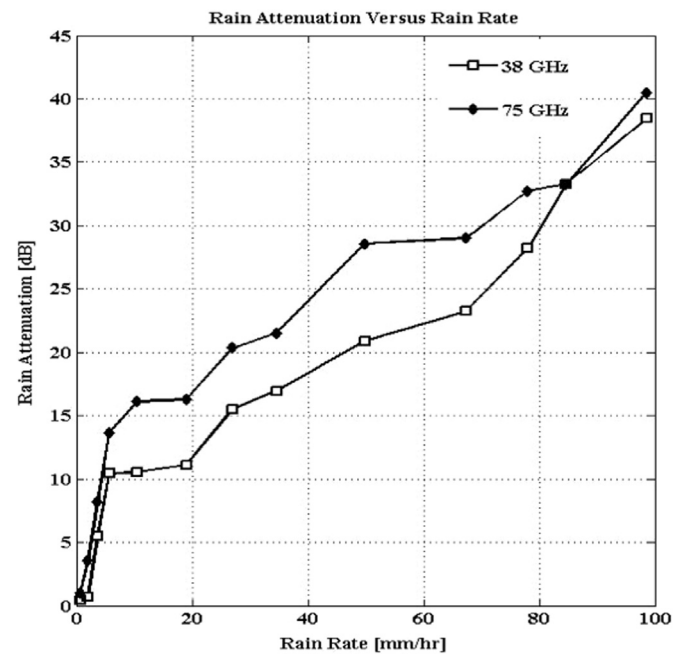


Fig. 3. Distribution of rain attenuation against rain rate (National Radio Research).

prediction error.

Fig. 5 depicts the equal probability plots of rainfall rates and ITU-R P. 530-16 prediction errors for 38 and 75 GHz under vertical polarization respectively. It also depicts that prediction error is more prominent for 75 GHz link as compared to 38 GHz. For instance, in 49.79 mm/h rain rate, the absolute errors obtained are 7.93 and 19.95 dB for 38 and 75 GHz link respectively. The error margins at 75 GHz link is better estimated by the polynomial function of fourth

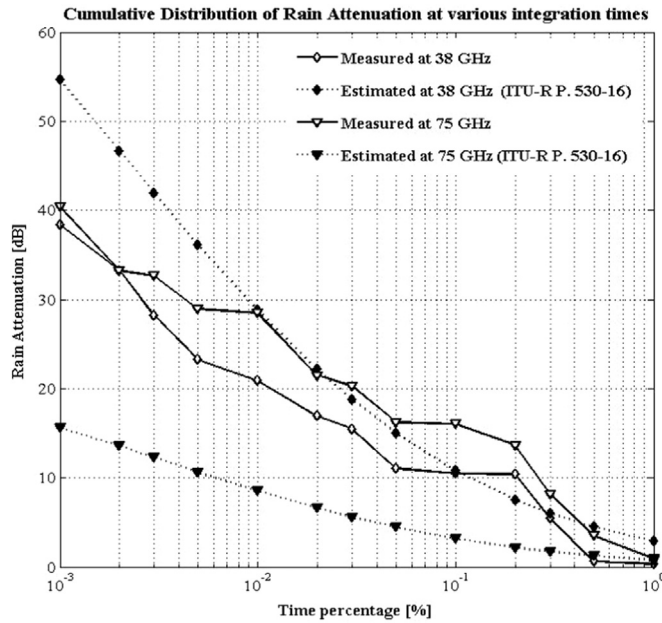


Fig. 4. Cumulative distribution of rain attenuation compared with ITU-R P. 530-16 for various integration times (www.mathworks.com).

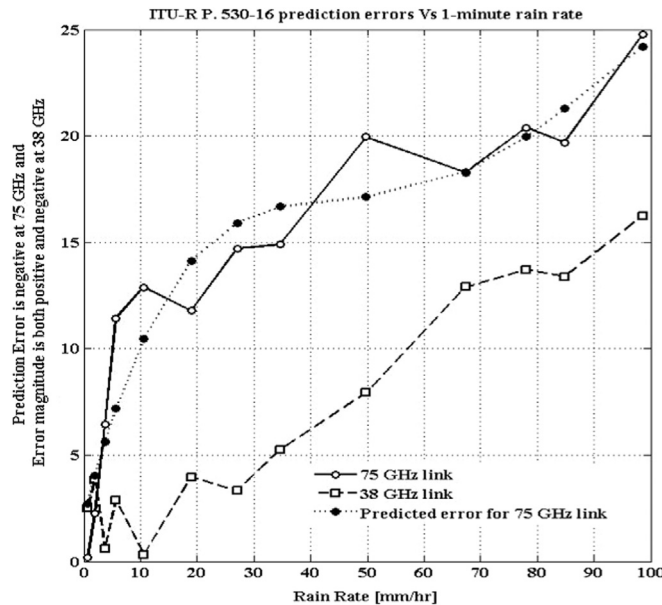


Fig. 5. Plot between predicted ITU-R P.530-16 error and 1-min. rainfall rate (www.mathworks.com).

order for vertical polarization respectively. For example, in 49.79 mm/h rain rate, the estimated error margin is 17.14 dB. This indicates that ITU-R P. 530-16 model performance statistics shows good agreement with calculated 1 min rain attenuation distribution from experimental 10-seconds measured rain attenuation values for 38 GHz link whereas underestimation is observed in 75 GHz link. In this concern, there is the need for 1 min rain attenuation prediction model that can give higher efficiency against the local 1 min rain attenuation distribution for terrestrial microwave links. The paper analyzes prominent rain

attenuation models along with ITU-R P. 530-16 that shall be applicable in the South Korea regions.

The deviation $\Delta A_{\%p}$ (dB) which is the ITU-R P.530-16 (ITU-R P. 530-16, 2015) prediction error against the measured rain attenuation values. Investigation of prediction error have shown that polynomial of fourth order is the best least square regression that fits the ITU-R P. 530-16 prediction error against the 1 min rain rate distribution for vertical polarization which is given as:

$$\Delta A_{\%p} = a_1 R_{\%p}^4 + a_2 R_{\%p}^3 + a_3 R_{\%p}^2 + a_4 R_{\%p} + a_5 \quad (4)$$

where, $\Delta A_{\%p}$ is the ITU-R P. 530-16 prediction error for vertical polarization and a_1, a_2, a_3, a_4, a_5 are regression parameters whose values depend on frequency and radio path length of the microwave link under consideration. Table 3 shows the values of regression coefficients used for the estimation of ITU-R P. 530-16 prediction errors against the full 1 min rain rate distribution over $0.001\% \leq p \leq 1\%$.

Hence, in order to improve ITU-R P. 530-16 rain attenuation prediction model, it is proposed that for vertical polarization Eq. (4) should be added to the predicted values as shown in proposed approach over the percentages of time, p , in the range 0.001–1% which is listed in Eq. (5):

$$A_{\%p}^{\text{predicted}} = A_{0.01} C_1 p^{-(C_2 + C_3 \log_{10} p)} + [a_1 R_{\%p}^4 + a_2 R_{\%p}^3 + a_3 R_{\%p}^2 + a_4 R_{\%p} + a_5] \quad (5)$$

where, $A_{0.01}$ is the estimated path attenuation exceeded for 0.01% of the time whose expression is defined in ITU-R P. 530-16 (ITU-R P. 530-16, 2015) model along with C_1, C_2 and C_3 terms.

Fig. 6(a)–(b) shows the plot for 38 and 75 GHz link with the application of prominent rain attenuation models. Due to the dependency on the experimental system, the derived coefficients as listed in Table 3 are tested for mentioned location and promising results are obtained to support the utilization of higher microwave frequencies. Further section clarifies the scientific argument to support the finding.

As noticed from Fig. 6(a)–(b), ITU-R P.530-16, Da Silva Mello, Abdulrahman et al. models follow closer with the measured cumulative statistics of rain attenuation for 38 GHz link and more closest is shown by Abdulrahman et al. Similarly, for 75 GHz link, the prediction errors between measured rain attenuation values and the ITU-R P. 530-16 predictions are less as compared to other models. So, addition of suitable prediction error margin to ITU-R P. 530-16 as depicted by proposed approach is suitable for the application in 75 GHz link. The Da Silva Mello shows excessive overestimation in 75 GHz link. For instance, Da Silva Mello predicts 15.82, 317.41, 1190.09 dB at 0.1%, 0.01%, 0.001% of the time so, this method is not depicted in Fig. 6(b). Moupfouma results in higher overestimation throughout the time percentage for 38 GHz but it largely underestimate in 75 GHz link. In addition, Lin and Differential Equations results in similar pattern and shows predictable accuracy at higher time percentage when $P \geq 0.5\%$ whereas for lower time percentage they shows overestimation for 38 GHz link. In contrast, higher underestimation is observed in 75 GHz link by the application of these methods. Table 4 depicts the measured and predicted rain attenuation values for 38 and 75 GHz links in 0.1, 0.01, 0.001% of the time. The proposed values at the end of the column indicate the obtained rain attenuation at 75 GHz link which is calculated from the Eq. (5) that shows the closer estimation against the measured values.

The goodness of fit for the proposed methods are done through the

Table 3
Regression coefficients for 75 GHz link.

Frequency (GHz)	Polarization	a_1	a_2	a_3	a_4	a_5
75	Vertical	−0.000001125	0.0003037	−0.02742	1.054	2.063

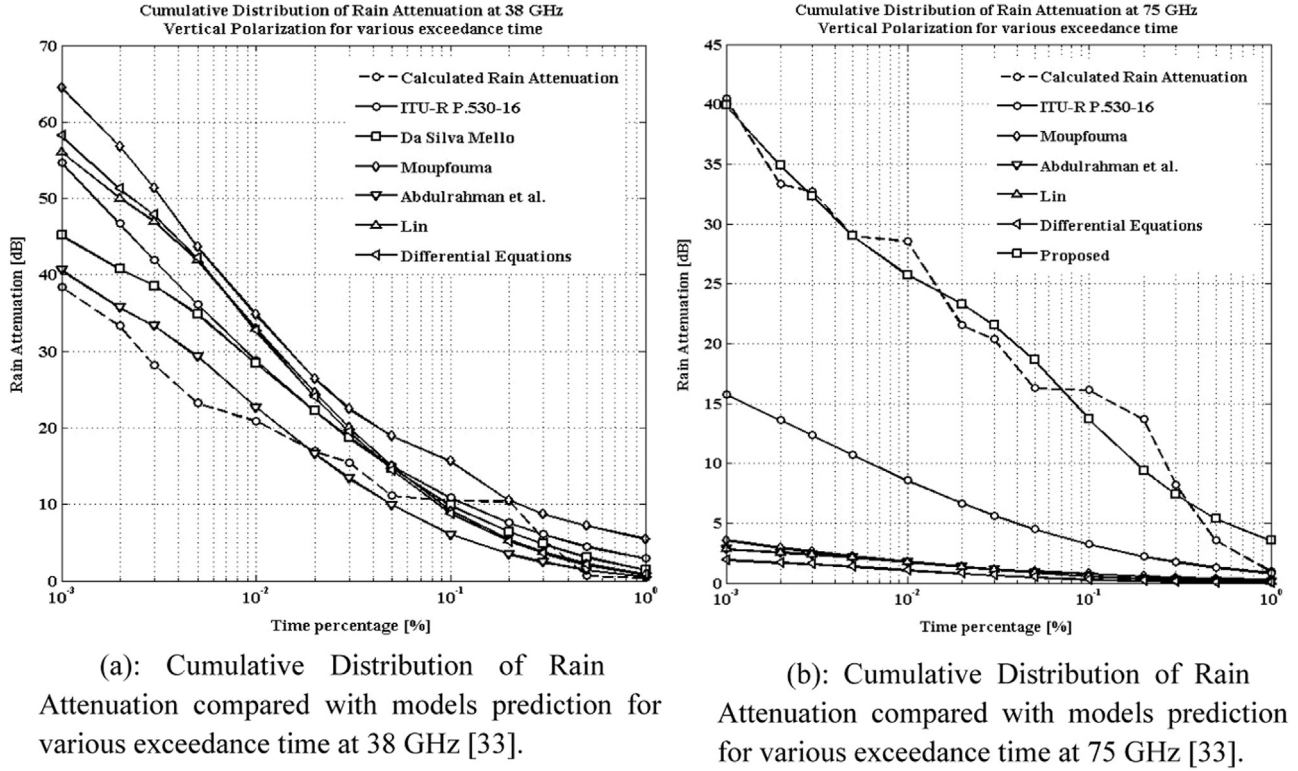


Fig. 6. (a): Cumulative Distribution of rain attenuation compared with models prediction for various exceedance time at 38 GHz (www.mathworks.com). (b): Cumulative distribution of rain attenuation compared with models prediction for various exceedance time at 75 GHz (www.mathworks.com).

calculation of relative error variables ($\varepsilon(P)$), Standard Deviation (STD) and Root Mean Square (RMS) values, where they are compared to the performance of the ITU-R P. 530-16, Da Silva Mello, Moupfouma and Abdulrahman et al., Lin and differential equations approaches. Data for prominent methods are tabulated at fixed probability levels when $0.001\% \leq p \leq 1\%$ as recommended in ITU-R P. 311-15 (ITU-R, 2015). The relative error probability used to access the proposed methods is given by:

$$\varepsilon(P)_T = \frac{A_{\%p, \text{predicted}} - A_{\%p, \text{measured}}}{A_{\%p, \text{measured}}} \times 100[\%] \quad (6)$$

where, $A_{\%p, \text{predicted}}$ and $A_{\%p, \text{measured}}$ are the predicted and measured rain attenuation values respectively, at the same probability level P , in the percentage interval $10^{-3}\% \leq P \leq 1\%$. Similarly, for STD and RMS calculation, the approaches followed in (Sujaan et al., 2016) have been adopted. The calculated relative error probability, $\varepsilon(P)$, Standard Deviation, STD, and Root Mean Square, RMS values of the test variable along with the mean (μ_v), standard deviation (σ_v) and root mean square (ρ_v) as recommended by ITU-R P.311-15 (Shrestha and Choi, 2016) for each method are listed in Table 5(a)-(b) for 38 and 75 GHz links under vertical polarization respectively. The fitted distributions were compared to the experimental values at time percentage 0.001–1%, using the test variable V_i as given by Eq. (7) and defined by ITU-R P. 311-15 (ITU-R, 2015) for each of the radio links.

$$V_i = \begin{cases} \left(\frac{A_{m,i}}{10}\right)^{0.2} \ln\left(\frac{A_{p,i}}{A_{m,i}}\right) & \text{for } A_{m,i} < 10\text{dB} \\ \ln\left(\frac{A_{p,i}}{A_{m,i}}\right) & \text{for } A_{m,i} \geq 10\text{dB} \end{cases} \quad (7)$$

where, A_m (dB) is the measured attenuation and A_p (dB) is the predicted attenuation. To evaluate the results over a range of time percentages, the σ_v and ρ_v values of all V_i values in the range is calculated.

As noted from Table 5(a) and (b), Da Silva Mello, Moupfouma, Lin,

Differential Equations shows higher relative error when $0.5\% \leq P \leq 1\%$ for 38 GHz whereas the relative error get higher as compared to ITU-R P. 530-16 for 75 GHz link which is justified from increased STD and RMS values. Under 38 GHz, Abdulrahman et al. show lower relative error for higher time percentage and for lower time percentage, ITU-R P.530-16, Da Silva Mello, Moupfouma, Abdulrahman et al., Lin, Differential Equations give higher relative error values which over-estimate the measured cumulative rain attenuation statistics. Thus, for 38 GHz link, ITU-R P. 530-16, Da Silva Mello and Abdulrahman et al. shows the closer estimation against the measured rain attenuation and more better is estimated by Abdulrahman et al. method. Similarly for 75 GHz link, ITU-R P. 530-16 shows lower relative error throughout the time percentage which is supported from lower STD and RMS values. Interestingly, addition of suitable deviation margin to the ITU-R P. 530-16 as shown by proposed method resulted in decreased error probabilities when $0.001\% < P < 1\%$. ITU-R P. 530-16, Da Silva Mello, Moupfouma, Abdulrahman et al., Lin, Differential Equations underestimate the measured cumulative rain attenuation statistics. In addition, Da Silva Mello shows greater overestimation against the calculated rain attenuation statistics which is justified from increased STD and RMS values. Thus, purposed approach can better estimate the rain attenuation statistics for $0.001\% < P < 1\%$. The tabulated values at 0.1%, 0.01% and 0.001% of the time support the finding at both millimeter wave bands. Furthermore, from the calculation of μ_v , as per the recommendation of ITU-R P.311-15, ITU-R P. 530-16, Da Silva Mello and Abdulrahman et al. result in relatively lower values which are supported by lower values of σ_v and ρ_v which justified their suitability for the estimation of rain attenuation in higher microwave frequencies band, particularly for 38 GHz link. Similarly, for 75 GHz link, ITU-R P.311-15, ITU-R P.530-16, Da Silva Mello, Moupfouma, Abdulrahman et al., Lin, Differential Equations result in higher μ_v values which are supported by higher values of σ_v and ρ_v . In contrast, the proposed approach gives lower μ_v values along with lower values of σ_v and ρ_v .

Furthermore, frequency scaling method is tested that provide an

Table 4
Attenuation values obtained for 0.1, 0.01, 0.001% of the time for 38 and 75 GHz links.

Time percentage [%]	Measured values at 38 GHz (dB)	ITU-R P. 530-16	Da Silva Mello	Moupfouma	Abdulrahman et al.	Lin	Differential equation	Measured values at 75 GHz (dB)	ITU-R P. 530-16	Moupfouma	Abdulrahman et al.	Lin	Differential equation	Proposed
0.1	10.53	10.85	9.86	15.65	6.03	9.19	8.82	16.11	3.22	0.81	0.58	0.59	0.59	13.71
0.01	20.89	28.83	28.42	34.85	22.68	33.04	32.71	28.55	8.59	1.78	1.74	1.77	1.77	25.74
0.001	38.44	54.67	45.19	64.54	40.66	56.09	58.21	40.48	15.71	3.59	2.83	2.87	2.87	39.9

alternative to rain attenuation models which are considered to be excellent predictors and provide a means for determining what to expect at a frequency for which there is no data. This paper analyses the approaches presented in ITU-R P. 530-16 (ITU-R P. 530-16, 2015) where the frequency scaling formula is adopted for estimation of rain attenuation at 75 GHz link under vertical polarization from the calculated 38 GHz rain attenuation values. However, the formulations given in the ITU-R P.530-16 is valid for frequencies in the range 7–50 GHz with the same hop length which has been used for the rough estimate of the attenuation statistics for 75 GHz link. Due to the limitation in experimental setup, with the fixed hop length of 3.2 km and 0.1 km for 38 and 75 GHz links respectively, the estimation of rain attenuation statistics from frequency scaling approach cannot be analyzed for the same hop length. Moreover, the rough estimation have been calculated which is depicted in the Fig. 7.

As noticed from Fig. 7, the estimated attenuation values are higher than the measured values for the 75 GHz link expect for the time percentage higher than 0.4% of the time. This might be due to the application of frequency scaling approach for two different hop lengths. We have used the measured attenuation statistics at 38 GHz link for 3.2 km hop length as input parameters for the frequency scaling method so as to estimate the rough attenuation values at 75 GHz link, irrespective of the consideration of normalization of 100 m hop length for 75–3.2 km hop length for 38 GHz links. For instance, the calculated rain attenuation values at 75 GHz link are 16.11, 28.55, 40.48 dB at 0.1%, 0.01% and 0.001% of the time and the estimated values after frequency scaling are 17.05, 30.89, 50.65 dB respectively. The better performance analyses are judged through the error matrices presented in Table 6.

As noticed from Table 6, the predicted 75 GHz rain attenuation statistics shows the less relative error chances for all time percentage when $0.001\% \leq P \leq 1\%$ of the time. This is justified from the lower STD, RMS, μ_v , σ_v and ρ_v values as per the ITU-R P. 311-15 which shows the applicability of the frequency scaling technique as mentioned in ITU-R P.530-16.

5. Conclusion

Based on the experimental setup for 38 and 75 GHz links, the rain attenuation and rain rate are measured simultaneously at these specific frequencies. Under these test conditions, ITU-R P. 530-16 shows closer estimation against measured rain induced attenuation particularly in 38 GHz whereas, in 75 GHz, ITU-R P. 530-16 shows relatively less prediction error and better estimation is observed by adding suitable deviation margin to its prediction method. Comparison of rain attenuation was made with the calculated rain attenuation distribution and six preexisting models. It is seen that although each of the models shows similar features at lower exceedance of time, the characteristic at higher time percentage highlight the quantitative difference from the experimental data in 38 GHz link. It was found that for 38 GHz link, ITU-R P.530-16, Da Silva Mello, Abdulrahman et al. models follow closer with the measured cumulative statistics of rain attenuation and more particularly, Abdulrahman et al. give closest values. Similarly, for 75 GHz link, ITU-R P. 530-16 and proposed approach shows reasonable estimation which is justified from the lower values of relative error, Standard Deviation and Root Mean Square error. In addition, the error analyses have been done through the application of ITU-R P.311-15 recommendation, which show the similar judgment for ITU-R P. 530-16, Da Silva Mello, Abdulrahman et al. models. However, proposed approach needs more validation and test from other regions of the South Korea with longer experimental observation periods that is helpful for reliable prediction method of rain attenuation. Furthermore, frequency scaling scheme is analyzed as per the recommendation of ITU-R P. 530-16 where the validation of this approach is performed by comparing with experimental data through error matrices.

Table 5

(a): Percentage error obtained after testing over the interval [0.001–1%] for 38 GHz under Vertical polarization.

Methods	Parameters	Time percentage (%)p										ITU-R P.311-15					
		1	0.5	0.3	0.2	0.1	0.05	0.03	0.02	0.01	0.005	0.003	0.002	0.001	μ_v	σ_v	ρ_v
ITU-R P. 530–16	$\varepsilon(P)$	6.21	5.76	0.11	−0.27	0.03	0.36	0.21	0.31	0.38	0.55	0.49	0.40	0.42	0.35	0.36	0.51
	STD	5.06	4.61	1.04	1.43	1.12	0.79	0.94	0.84	0.77	0.60	0.66	0.75	0.73			
	RMS	2.53	3.84	0.59	2.87	0.32	3.98	3.33	5.26	7.93	12.90	13.72	13.37	16.23			
Da Silva Mello	$\varepsilon(P)$	2.54	3.68	−0.12	−0.39	−0.06	0.33	0.21	0.31	0.36	0.50	0.37	0.23	0.18	0.23	0.33	0.4
	STD	1.92	3.06	0.75	1.01	0.69	0.30	0.42	0.32	0.27	0.12	0.26	0.40	0.45			
	RMS	1.04	2.46	0.66	4.05	0.67	3.63	3.23	5.24	7.52	11.63	10.34	7.49	6.75			
Moupfouma	$\varepsilon(P)$	12.59	9.85	0.60	0.01	0.49	0.82	0.71	0.45	0.67	0.88	0.82	0.71	0.68	0.59	0.37	0.7
	STD	10.36	7.61	1.63	2.22	1.74	1.52	1.78	1.67	1.56	1.35	1.41	1.52	1.55			
	RMS	5.12	6.56	3.28	0.09	5.12	7.85	7.03	9.50	13.95	20.39	23.21	23.55	26.10			
Abdulrahman et al.	$\varepsilon(P)$	0.36	1.16	−0.55	−0.66	−0.43	−0.10	−0.13	−0.02	0.09	0.26	0.18	0.07	0.06	−0.11	0.41	0.43
	STD	0.34	1.14	0.57	0.69	0.45	0.13	0.15	0.04	0.06	0.24	0.16	0.05	0.04			
	RMS	0.36	1.16	0.55	0.66	0.43	0.10	0.13	0.02	0.09	0.26	0.18	0.07	0.06			
Lin	$\varepsilon(P)$	0.92	2.33	−0.31	−0.48	−0.13	0.35	0.30	0.45	0.58	0.80	0.66	0.50	0.46	0.25	0.37	0.45
	STD	0.42	1.84	0.80	0.98	0.62	0.14	0.20	0.04	0.08	0.31	0.17	0.01	0.04			
	RMS	0.37	1.56	1.68	5.05	1.33	3.94	4.61	7.71	12.14	18.66	18.77	16.75	17.64			
Differential equations	$\varepsilon(P)$	1.03	2.20	−0.34	−0.51	−0.16	0.31	0.26	0.42	0.57	0.81	0.69	0.54	0.51	0.24	0.39	0.46
	STD	0.54	1.72	0.82	0.99	0.65	0.18	0.23	0.07	0.08	0.33	0.21	0.05	0.03			
	RMS	0.42	1.47	1.83	5.28	1.71	3.40	4.02	7.13	11.82	18.95	19.59	17.95	19.76			

(b): Percentage error obtained after testing over the interval [0.001–1%] for 75 GHz under Vertical polarization.

Methods	Parameters	Time percentage (%)p										ITU-R P.311-15					
		1	0.5	0.3	0.2	0.1	0.05	0.03	0.02	0.01	0.005	0.003	0.002	0.001	μ_v	σ_v	ρ_v
ITU-R P. 530–16	$\varepsilon(P)$	−0.18	−0.64	−0.78	−0.84	−0.80	−0.72	−0.72	−0.69	−0.70	−0.63	−0.62	−0.59	−0.61	−1.12	0.4	1.19
	STD	0.48	0.02	0.13	0.18	0.14	0.07	0.07	0.04	0.04	0.03	0.03	0.06	0.04			
	RMS	0.18	2.27	6.45	11.44	12.89	11.78	14.71	14.89	19.95	18.28	20.38	19.68	24.77			
Da Silva Mello	$\varepsilon(P)$	−0.93	−0.83	−0.75	−0.66	−0.02	2.03	3.78	6.31	10.12	18.64	22.18	25.69	28.40	1.1	1.89	2.19
	STD	9.70	9.59	9.51	9.43	8.79	6.74	4.98	2.46	1.35	9.87	13.41	16.92	19.63			
	RMS	0.94	2.95	6.13	9.01	0.30	32.98	76.99	135.90	288.86	540.34	725.49	855.42	1149.62			
Moupfouma	$\varepsilon(P)$	−0.72	−0.89	−0.95	−0.96	−0.95	−0.94	−0.94	−0.94	−0.94	−0.92	−0.91	−0.91	−0.91	−2.52	0.59	2.59
	STD	0.19	0.02	0.03	0.05	0.04	0.02	0.03	0.02	0.02	0.01	0.00	0.00	0.00			
	RMS	0.73	3.19	7.77	13.12	15.30	15.27	19.23	20.15	26.77	26.73	30.06	30.35	36.89			
Abdulrahman et al.	$\varepsilon(P)$	−0.92	−0.95	−0.97	−0.97	−0.96	−0.95	−0.94	−0.94	−0.94	−0.93	−0.93	−0.92	−0.93	−2.78	0.47	2.81
	STD	0.02	0.01	0.02	0.03	0.02	0.00	0.00	0.00	0.00	0.02	0.02	0.02	0.01			
	RMS	0.93	3.39	7.94	13.30	15.53	15.40	19.22	20.19	26.81	26.83	30.32	30.76	37.65			
Lin	$\varepsilon(P)$	−0.92	−0.95	−0.97	−0.97	−0.96	−0.95	−0.94	−0.94	−0.94	−0.92	−0.93	−0.92	−0.93	−2.76	0.47	2.8
	STD	0.02	0.01	0.02	0.03	0.02	0.00	0.00	0.00	0.00	0.02	0.02	0.02	0.02			
	RMS	0.93	3.39	7.94	13.30	15.53	15.38	19.20	20.17	26.78	26.80	30.28	30.72	37.61			
Differential equations	$\varepsilon(P)$	−0.97	−0.98	−0.99	−0.99	−0.98	−0.97	−0.97	−0.96	−0.96	−0.95	−0.95	−0.95	−0.95	−2.76	0.47	2.8
	STD	0.01	0.01	0.02	0.02	0.01	0.00	0.00	0.00	0.01	0.02	0.02	0.02	0.02			
	RMS	0.98	3.50	8.10	13.50	15.82	15.80	19.70	20.74	27.46	27.58	31.12	31.59	38.53			
Proposed	$\varepsilon(P)$	2.54	0.50	−0.10	−0.31	−0.15	0.14	0.06	0.08	−0.10	0.00	−0.01	0.05	−0.01	0.05	0.27	0.27
	STD	2.33	0.29	0.31	0.52	0.36	0.06	0.15	0.12	0.30	0.21	0.22	0.16	0.22			
	RMS	2.56	1.78	0.83	4.26	2.40	2.36	1.21	1.79	2.81	0.02	0.43	1.60	0.57			

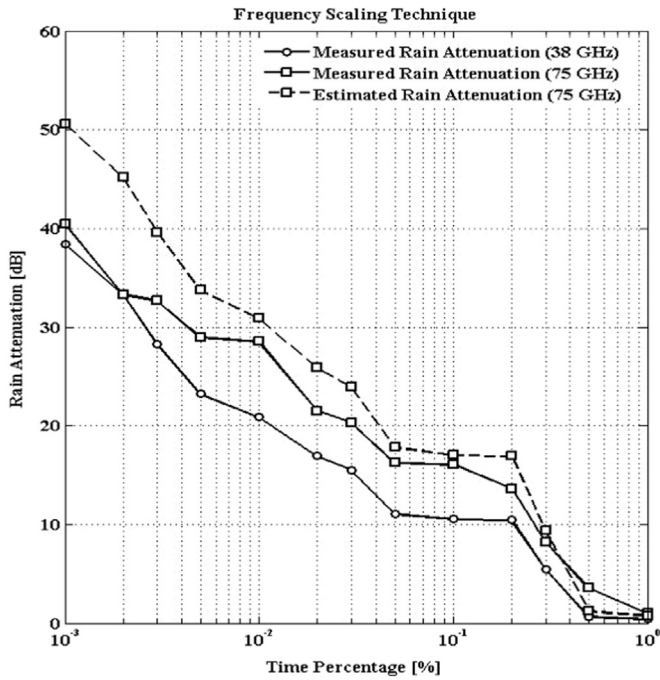


Fig. 7. Cumulative distribution of calculated and estimated rain attenuation obtained after frequency scaling technique.

From the statistical analysis of rain rate and rain attenuation data,

it can be concluded that the ITU-R P. 530-16 shows reasonable estimation behavior of the propagation measurement systems. The results of two sets of data can be used to understand the behavior of signal propagation of rain in this region. However, in order to obtain a consistent and accurate data, long-term data is essential. In overall, the ITU-R P. 530-16 seems to be suitable but it need to be analyzed further for better prediction by collecting data of longer periods as well as from other location of the South Korea. This contribution presented an overview of the research activities aimed to model rain induced attenuation to cope with severe atmospheric propagation impairments experienced by high-frequency wireless systems.

Competing interests

The authors declare that they have no competing interests.

Acknowledgements

This study was supported by research fund from Chosun University, 2016.

Appendix A

Model

ITU-R P. 530–16 (ITU-R P, 2015)

Da Silva Mello (da Silva Mello et al., 2007; Mello and Pontes, 2012)

Moupfouma (Moupfouma, 2009)

Abdulrahman et al. Abdulrahman et al., (2011)

Lin (Lin, 1977)

Differential equation approach

Factors

Distance factor, r

$$r = \frac{1}{0.477d^{0.633}R_{0.01}^{0.073}a^{0.123} - 10.579(1 - \exp(-0.024d))}$$

Path reduction factor, $r = \frac{1}{1 + \left(\frac{d}{d_0(R_p)}\right)}$

where,

$$\phi(a) = \left(\frac{a}{A_{0.01}} - 1\right) \times \ln\left(1 + \frac{a}{A_{0.01}}\right) \text{ and}$$

$$\eta(a) = \frac{1}{1 + 2.75 \times \left(\frac{a}{A_{0.01}}\right)^{0.8}}$$

Path reduction factor, $\delta(R_{0.01}, d) =$

$$\frac{1}{1 + \left(\frac{d}{2.6379 \times R_{0.01}^{0.21}}\right)}$$

Path reduction factor, r

$$r = \frac{1}{1 + \left(\frac{L}{L(R)}\right)} \text{ where, } L(R) = \frac{2636}{R - 6.2}$$

where, $\beta = k[\alpha + b(1 - r_{\%p})]d_{\text{eff}}$ and

Attenuation exceeded [0.001–1%]

$$\frac{A_p}{A_{0.01}} = C_1 p^{-(C_2 + C_3 \log_{10} p)}$$

$$A = \gamma_R d_{\text{eff}} = k [R_{\text{eff}}(R_p, d)]^a \left[\frac{1}{1 + \left(\frac{d}{d_0(R_p)}\right)} \right] \times d$$

$$P(A_{0.01} \geq a) = 0.01 \times \left(\frac{A_{0.01} + 1}{a + 1}\right)^{\phi(a)} \times \exp\left(9.21 \times \left(1 - \frac{a}{A_{0.01}}\right) \times \eta(a)\right)$$

$$A_{\%p} = \gamma_R d_{\text{eff}} = \{k(R_{\%p})^a\} * \frac{d}{1 + \left(\frac{d}{2.6379 * R_{0.01}^{0.21}}\right)}$$

$$A_{\%p} = \gamma_R d_{\text{eff}} = \{k(R_{\%p})^a\} * \frac{d}{1 + \left(\frac{L}{L(R)}\right)}$$

$$A_{\%p} = \mu [S(R_{\%p})] \text{ and, } S(R_{\%p}) = \beta (R_{\%p})^{\alpha-1}$$

Table 6

Percentage error obtained after testing over the interval [0.001–1%] after frequency scaling technique.

Methods	Parameters	Time percentage (%)													ITU-R P.311-15		
		1	0.5	0.3	0.2	0.1	0.05	0.03	0.02	0.01	0.005	0.003	0.002	0.001	μ_v	σ_v	ρ_v
ITU-R P. 530–16 (Frequency scaling- estimated 75 GHz)	$\varepsilon(P)$	−0.23	−0.65	0.14	0.24	0.06	0.10	0.18	0.20	0.08	0.17	0.21	0.36	0.25	0.06	0.28	0.29
	STD	0.31	0.73	0.06	0.15	0.03	0.01	0.09	0.12	0.00	0.08	0.13	0.27	0.17			
	RMS	0.23	2.31	1.18	3.26	0.93	1.59	3.61	4.34	2.35	4.80	6.91	11.94	10.17			

(Abdulrahman et al., 2012b)

$$\mu = \frac{R_{\%p}}{\alpha + b(1 - r_{\%p})}$$

References

- Crane, Robert K., 1996. *Electromagnetic Wave Propagation through Rain*. John Wiley & Sons Series, UK.
- Freeman, R.L., 2007. *Radio System Design for Telecommunication* 3rd edition. A Wiley Inter-science Publication, Wiley, John Wiley & Sons Inc., San Francisco, United States.
- Kanellopoulos, John D., et al., 1990. Rain Attenuation Problems Affecting the Performance of Microwave Communication Systems. *Annales des Télécommunication* 45. Springer-Verlag, Netherland.
- Mandeep, J.S., Hassan, S.I.S., Ain, M.F., 2008. Rain rate conversion for various integration time for equatorial and tropical climates.. *Int. J. Satell. Commun. Netw.* 26.4, 329–345.
- Barclay, Leslie W., 2003. *Propag. Radio*. 502, (Iet).
- Sujan, Shrestha, Park, Jung-Jin, Choi, Dong-You, 2016. Rain rate modeling of 1 min from various integration times in South Korea. *SpringerPlus* 5, 1.
- Shrestha Sujan, Park Jung-Jin, Kim, S.W., Kim J.J., Jung J.H., Choi, D.Y., (2016), 1 min Rain Rate Derivation from Various Integration Times in South Korea. Korean Institute of Next Generation Computing, January, Bangkok, Thailand.
- Choi, D.Y., Pyun, J.Y., Noh, S.K., Lee, S.W., 2012. Comparison of measured rain attenuation in the 12.25-GHz band with predictions by the ITU-R model., (Article ID 415398) *Int. J. Antennas Propag.* 2012, 1–5.
- Islam, Rafiqul M.D., Yusuf, A. Abdulrahman, Tharek, A. Rahman, 2012. An improved ITU-R rain attenuation prediction model over terrestrial microwave links in tropical region. *EURASIP J. Wirel. Commun. Netw.* 2012.1, 1–9.
- IO, Yussuff Abayomi, 2016. Babatunde Olusegun, and Nor Hisham Haji Khamis. "Comparative Analysis of Terrestrial Rain Attenuation at Ku band for Stations in South-Western Nigeria."
- Kesavan, Ulaganathen, et al., 2011. Comparative studies of the rain attenuation predictions for tropical regions. *Prog. Electromagn. Res.* M18, 17–30.
- Mandeep, Jit Singh, 2009. Rain attenuation statistics over a terrestrial link at 32.6 GHz at Malaysia. *Microw. Antennas Propag. IET* 3.7, 1086–1093.
- Abdulrahman, A.Y., et al., 2012a. Rain attenuation measurements over terrestrial microwave links operating at 15 GHz in Malaysia. *Int. J. Commun. Syst.* 25.11, 1479–1488.
- Abdulrahman, Amuda Yusuf, et al., 2011. Comparison of measured rain attenuation and ITU-R predictions on experimental microwave links in Malaysia. *Int. J. Microw. Wirel. Technol.* 3.04, 477–483.
- Abdulrahman, Yusuf A., et al., 2016. Statistical Evaluation of measured rain attenuation in tropical climate and Comparison with prediction models. *J. Microw., Optoelectron. Electromagn. Appl.* 15.2, 123–134.
- Hirata, Akihiko, et al., 2009. Effect of rain attenuation for a 10-Gb/s 120-GHz-band millimeter-wave wireless link. *IEEE Trans. Microw. Theory Tech.* 57.12, 3099–3105.
- ITU-R P. 530-16, 2015. Propagation data and prediction methods required for the design of terrestrial line-of-sight systems, ITU, Geneva, Switzerland.
- da Silva Mello, L.A.R., et al., 2007. Prediction of rain attenuation in terrestrial links using full rainfall rate distribution. *Electron. Lett.* 43.25, 1442–1443.
- Mello, L., Pontes, Marlene S., 2012. Unified method for the prediction of rain attenuation in satellite and terrestrial links. *J. Microw., Optoelectron. Electromagn. Appl.* 11.1, 01–14.
- Moupfouma, Fidèle, 2009. Electromagnetic waves attenuation due to rain: a prediction model for terrestrial or LOS SHF and EHF radio communication links. *J. Infrared, Millim. Terahertz Waves* 30.6, 622–632.
- Abdulrahman, A.Y., et al., 2011. Empirically derived path reduction factor for terrestrial microwave links operating at 15 GHz in Peninsula Malaysia. *J. Electromagn. Waves Appl.* 25.1, 23–37.
- Lin, S.H., 1977. 11-GHz radio: nationwide long-term rain rate statistics and empirical calculation of 11-GHz microwave rain attenuation. *Bell Syst. Tech. J.* 56.9, 1581–1604.
- Abdulrahman, A.Y., et al., 2012b. Rain attenuation predictions on terrestrial radio links: differential equations approach. *Trans. Emerg. Telecommun. Technol.* 23.3, 293–301.
- COST 255, Final Document Report on Radiowave Propagation modeling for new satellite communication services at Ku Band and above.
- Korea Meteorological Administration (KMA), (web.kma.go.kr/eng/index.jsp)
- Kestwal, Mukesh Chandra, Sumit Joshi, and Lalit Singh Garia, (2014). Prediction of rain attenuation and impact of rain in wave propagation at microwave frequency for tropical region (Uttarakhand, India). *Int. J. Micro. Sci. Technol.* 2014.
- Crane, Robert K., 2003. *Propagation handbook for wireless communication system design*. CRC press, UK.
- ITU-R, 2005. Specific Attenuation Model for Rain for Use in Prediction Methods, Recommendation P.838-3, ITU-R Recommendations, P Series, ITU, Geneva, International Telecommunications Union.
- ITU-R Databank DBSG3, (<http://www.itu.int/pub/R-SOFT-SG3/en>)
- National Radio Research Agency (RRA) 767, Bitgaram-ro, Naju-si, Jeollanam-do 58217, Republic of Korea (<http://www.rra.go.kr/en/index.jsp>)
- (<http://www.ott.com>)
- OTT, Operating Instructions: Present Weather Sensor Parsivel, 70.200.005.B.E 08-1008. (www.mathworks.com), the Mathworks, Inc., Protected by U.S. and International Patents.
- ITU-R, 2015. P. 311-15, Acquisition, Presentation and Analysis of Data in Studies of Radio Wave Propagation, International Telecommunication Union, Geneva.
- Shrestha, Sujan, Choi, Dong-You, 2016. Study of rain attenuation in Ka band for satellite communication in South Korea. *J. Atmos. Sol.-Terr. Phys.* 148, 53–63.
- Sujan, Shrestha, Choi, Dong-You, 2016. Proposed one-minute rain rate Conversion method for microwave applications in South Korea. *J. Inf. Commun. Converg. Eng.* 14 (3). <http://dx.doi.org/10.6109/jicce.2016.14.3.153>, (August).